New Physical Discrete UHF Multilayer Propagation Model for Urban Areas

S. Selim Seker [1], Gokhan Apaydin [1,2]

[1] Department of Electrical and Electronic Engineering,
Bogazici University, 34340, Istanbul, Turkey, email: seker@boun.edu.tr
[2] Applied Research and Development, University of Technology Zurich,
Technoparkstrasse 1, 8005, Zurich, Switzerland, e-mail: gapaydin@hsz-t.ch

Abstract **–** In this paper, a newly developed discrete multilayer propagation model using scattering theory is studied using rectangular lossy multilayer dielectric plates which model the walls, the streets, and avenues in urban areas. The model is presented to study radio wave propagation in street environments and to compare it with previous theoretical and experimental studies. Good agreements are found. Using the developed model, it is possible to calculate the contributions of direct and scattered wave separately. The simulations reveal that the developed model can be applicable for a broad band of frequencies. This model can be used effectively for prediction of loss characteristics in a situation when two antennas are located below the rooftops in conditions of direct visibility.

Key words **–** Discrete model, path loss, urban areas, scattering, multilayer propagation model.

I. INTRODUCTION

There are many propagation models of Electromagnetic (EM) waves propagating in various kinds of building structures with differing shapes. The field of modeling has been extensively studied over the last decade. The models are important for designers of urban wireless communication links, namely for a precise prediction of link budget and radio coverage of areas of services. For each kind of planar building structures, different mathematical models have been proposed and good approximations have been done by successful studies. The evaluation of "Multislit Street Waveguide Model" [1-2] is introduced to describe the propagation characteristics along straight rectangular streets in cases where all antennas, the receiver, and the transmitter are placed in direct visibility (Line Of Sight conditions) at lower than rooftop level. In the same study [1], the conditions of regular terrain are considered further in the obstructive conditions (No Line Of Sight) for antennas, and they are described in the case of urban environments with a rectangular crossing street plan for different positions of both antennas relative to the rooftops. Furthermore, "Crossing Waveguides Model" [1-2] and the "Two Dimensional Multi diffraction Model" [3] are presented to describe the propagation characteristics and the coverage effects. The frequency characteristics and propagation attenuation constant in straight open-groove structures are presented in [4]. Ray tracing technique is explained in [3-5]. Ray Theory and Uniform Theory of Diffraction (UTD) are used to predict wave strength. In [6], modeling and measurements of EM-wave propagation in the Berlin Subway is presented.

As it has been mentioned in [1], the path loss in a residential environment depends on the dielectric properties of structures. All of the studies in literature assume that the walls are planar. However, this is not the case in the real world.

The developed propagation model based on the scattering formulation for the streets, ground, and walls in urban areas, has been introduced consisting of rectangular lossy multilayer dielectric plates for EM-waves. The novelty in this paper is the usage of "Discretized approach for scattering field" from irregular or arbitrary dielectric surfaces, where no exact solution is available.

In section II, the discretized approach for scattering field is illustrated. In sections III and IV, verification of the method is acquired using the results from literature for the radar cross section (RCS) of tunnel. Development of model for urban areas and simulations are done in section V and VI. In conclusions, we present the advantages of the model compared to the earlier model of propagation.

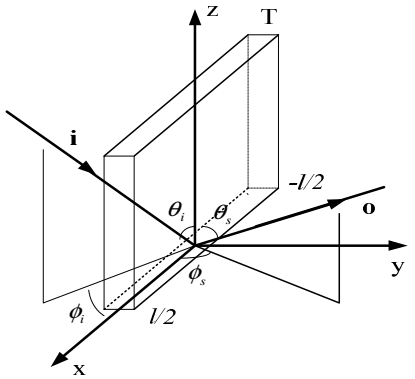

Fig. 1. Scattering from a dielectric sheet.

II. THE DISCRETIZED APPROACH FOR SCATTERING FIELD

The developed model is based on the determination of scattering amplitudes and scattering fields, introduced in [7] using scattering theory. The suggested method, which relies on the discretization approach, is valid only when curved surface is big compared to thickness in one direction. Firstly, the surface or shape is divided into multilayer rectangular plates. The scattering amplitudes and fields caused by each individual plate are calculated. Afterwards the contribution of each plate in the arbitrary shape is summed in an integral form to determine the scattering amplitudes for the whole surface or shape.

Consider an incident plane electromagnetic wave at an arbitrary dielectric surface representing multilayer plate seen in Fig. 1. The plane wave is assumed to have polarization ($\mathbf{p}$) and to be propagating in the $\mathbf{i}$ direction

$$\mathbf{E_i}(\mathbf{r}) = \mathbf{p}\, E_0\, e^{jk_0 \mathbf{i}\cdot\mathbf{r}}, \tag{1}$$

where E_0 is the magnitude of the incident wave, $\mathbf{r}$ is the general position vector, $k_0 = \omega\sqrt{\mu_0\varepsilon_0}$ is the free space wave number and the direction of incident wave is

$$-\mathbf{i} = \sin\theta_i\left(\cos\phi_i\hat{x} + \sin\phi_i\hat{y}\right) + \cos\theta_i\hat{z}\,. \tag{2}$$

In (2), the spherical angles of the incident wave (θ_i and φ_i) are measured with respect to polar axes z and x, respectively. Incident waves with both horizontal ($\mathbf{p} = \mathbf{h_i}$) and vertical ($\mathbf{p} = \mathbf{v_i}$) polarizations are taken into consideration. The horizontal polarization is $\mathbf{h_i} = (\mathbf{i}\times\hat{z})/|\mathbf{i}\times\hat{z}|$. The vertical polarization is taken perpendicular to both $\mathbf{i}$ and $\mathbf{h_i}$, thus $\mathbf{v_i} = \mathbf{h_i}\times\mathbf{i}$.

The formal solution for the scattered fields ($\mathbf{E}_s(\mathbf{o},\mathbf{i}) = \mathbf{f}(\mathbf{o},\mathbf{i})\dfrac{e^{jk_0R}}{R}$ where R is the distance between scatterer and observation point) from the surface can be obtained in terms of the fields inside the scatterer using a standard procedure [8]. The integral form of scattering amplitude is ($f_{pq}=\mathbf{p}\cdot\mathbf{f}\cdot\mathbf{q}$, $\mathbf{p}\in\{\mathbf{h_i},\mathbf{v_i}\}$, $\mathbf{q}\in\{\mathbf{h_o},\mathbf{v_o}\}$)

$$\begin{aligned}\mathbf{f}(\mathbf{o},\mathbf{i}) &= \frac{k_0^2}{4\pi}\int_{Vol}(\varepsilon_r(\mathbf{r}')-1)(\mathbf{I}-\mathbf{oo})\cdot\mathbf{E_{int}}(\mathbf{r}')\cdot e^{-jk_0\mathbf{o}\cdot\mathbf{r}'}d\mathbf{r}' \\ &= f_{hh}\mathbf{h_o}\mathbf{h_i} + f_{vh}\mathbf{v_o}\mathbf{h_i} + f_{hv}\mathbf{h_o}\mathbf{v_i} + f_{vv}\mathbf{v_o}\mathbf{v_i}\,,\end{aligned} \tag{3}$$

where $f_{hh}, f_{vh}, f_{hv}, f_{vv}$ are the scattering amplitudes, $\mathbf{I}$ is a unit dyadic, $\mathbf{o}$ is a unit vector towards an observation point, and $\mathbf{E_{int}}$, which is not known in general, is the internal field inside the scatterer or object. The integration is carried out over the volume of the scatterer. In terms of the scattering angles θ_s and φ_s, $\mathbf{o}$ is written as

$$\mathbf{o} = \sin\theta_s\left(\cos\varphi_s\hat{x} + \sin\varphi_s\hat{y}\right) + \cos\theta_s\hat{z}\,. \tag{4}$$

In order to solve (3), it is necessary to know the fields inside the scatterer which is the dielectric surface of street, wall or ground for this study. It is characterized by constitutive parameters: permittivity ($\varepsilon_0\varepsilon_r$) and permeability (μ_o) of the dielectric material. Next, we deal with the problem of finding the internal field of the surface.

The fields inside the rectangular plate sheet are the same as the ones that would exist in a multilayer dielectric slab of the same physical and geometrical properties. Thus the horizontal ($\mathbf{E^h}$) and vertical ($\mathbf{E^v}$) electric fields inside each layer can be expressed as:

$$\mathbf{E}_m^{\mathbf{h}} = A_m\, e^{-\gamma_m\cdot\mathbf{r}}\mathbf{q}_- + B_m\, e^{\gamma_m\cdot\mathbf{r}}\mathbf{q}_+, \quad \mathbf{q}\in\{\mathbf{h},\mathbf{v}\}, \tag{5}$$

$$\mathbf{E}_m^{\mathbf{v}} = F_m\, e^{-\gamma_m\cdot\mathbf{r}}\mathbf{q}_- + G_m\, e^{\gamma_m\cdot\mathbf{r}}\mathbf{q}_+, \quad \mathbf{q}\in\{\mathbf{h},\mathbf{v}\}, \tag{6}$$

where $\boldsymbol{\gamma}_m$ is the propagation constant in the m^{th} layer and A_m, B_m, F_m, G_m are coefficients of the plane wave for horizontal and vertical electric fields. An electromagnetic wave of any kind of polarization can be decomposed into its orthogonal linearly polarized components. The electric fields parallel to the interface are horizontally polarized and the fields perpendicular to the interface are vertically polarized.

Using boundary conditions, the coefficients for the horizontal and vertical polarized wave having an incident angle of each layer θ_m and layer position d_m upon a multilayer dielectric slab of n layers with a relative permittivity (ε_m), and the loss tangent ($\tan\delta_m$) are

$$\begin{bmatrix}A_m\\ B_m\end{bmatrix} = \frac{1}{2}\begin{bmatrix}(1+Y_{m+1})e^{(\gamma_{m+1}-\gamma_m)d_m} & (1-Y_{m+1})e^{-(\gamma_{m+1}+\gamma_m)d_m}\\ (1-Y_{m+1})e^{(\gamma_m+\gamma_{m+1})d_m} & (1+Y_{m+1})e^{(\gamma_m-\gamma_{m+1})d_m}\end{bmatrix}\begin{bmatrix}A_{m+1}\\ B_{m+1}\end{bmatrix}, \tag{7}$$

$$\begin{bmatrix}F_m\\ G_m\end{bmatrix} = \frac{1}{2}\begin{bmatrix}(1+W_{m+1})e^{(\gamma_{m+1}-\gamma_m)d_m} & (1-W_{m+1})e^{-(\gamma_{m+1}+\gamma_m)d_m}\\ (1-W_{m+1})e^{(\gamma_m+\gamma_{m+1})d_m} & (1+W_{m+1})e^{(\gamma_m-\gamma_{m+1})d_m}\end{bmatrix}\begin{bmatrix}F_{m+1}\\ G_{m+1}\end{bmatrix}, \tag{8}$$

where $Y_{m+1} = \dfrac{\cos\theta_{m+1}}{\cos\theta_m}\sqrt{\dfrac{\varepsilon_{m+1}(1-j\tan\delta_{m+1})}{\varepsilon_m(1-j\tan\delta_m)}}$, and $W_{m+1} = \dfrac{\cos\theta_{m+1}}{\cos\theta_m}\sqrt{\dfrac{\varepsilon_m(1-j\tan\delta_m)}{\varepsilon_{m+1}(1-j\tan\delta_{m+1})}}$ respectively.

After substituting (5) and (6) into (3), and evaluating the integral, scattering amplitudes for horizontal and vertical polarization are obtained as:

$$f_{hh} = \sum_{m=1}^{n}\left[\frac{{k_0}^2(\varepsilon_m - 1)S_m}{4\pi}\left(A_m\frac{e^{d_m C_m} - e^{d_{m-1}C_m}}{C_m} + B_m\frac{e^{-d_{m-1}D_m} - e^{-d_m D_m}}{D_m}\right)\right], \quad (9)$$

$$f_{vv} = \frac{{k_0}^2}{4\pi}(K_1\cos\theta_s - K_2\sin\theta_s), \quad (10)$$

where

$$K_1 = \sum_{m=1}^{n}\left[\frac{k_{m-1}(\varepsilon_m - 1)S_m}{k_0\,\varepsilon_m}\left(F_m\frac{e^{d_{m-1}C_m} - e^{d_m C_m}}{C_m} + G_m\frac{e^{-d_{m-1}D_m} - e^{-d_m D_m}}{D_m}\right)\right],$$

$$K_2 = \sin\theta_i\sum_{m=1}^{n}\left[\frac{(\varepsilon_m - 1)S_m}{\varepsilon_m}\left(F_m\frac{e^{d_m C_m} - e^{d_{m-1}C_m}}{C_m} + G_m\frac{e^{-d_{m-1}D_m} - e^{-d_m D_m}}{D_m}\right)\right],$$

$C_m = j(k_m + k_0\cos\theta_s)$, $D_m = j(k_m - k_0\cos\theta_s)$, $k_m = k_0\sqrt{\varepsilon_m - \sin^2\theta_i}$, S_m is the shape function, θ_s is the scattered angle, and n is the number of layers. The shape function for rectangular cross section is obtained as:

$$S_m = X_0 Y_0\, Sinc(k_0 X_o\sin\theta_m), \quad (11)$$

where X_0, Y_0 are the side lengths, and θ_m is the incident angle of each layer.

After determining the scattering amplitudes of multilayer rectangular plate, the scattering amplitude of an arbitrary dielectric surface is obtained as:

1. The arbitrary dielectric surface is divided into *N* small approximately rectangular strips, each of which has a center described by x_c, y_c, z_c. For each strip, the normal vector ($\mathbf{n_c}$) is determined ($c = 1, 2, ...N$).

2. The scattering amplitudes of each sheet $\mathbf{f}^{(c)}(\mathbf{o},\mathbf{i})$ are determined by using the multilayer model.

3. Each scattering amplitude is added coherently in order to obtain scattering amplitude of the total surface as, $\mathbf{f}(\mathbf{o},\mathbf{i}) = \sum_{c=1}^{N}\mathbf{f}^{(c)}(\mathbf{o},\mathbf{i})e^{jk_0\boldsymbol{\zeta}\cdot\mathbf{r}_c}$ where $\boldsymbol{\zeta} = \mathbf{i} - \mathbf{o}$ with $\mathbf{r}_c$ being the position vector to the center of the c^{th} strip.

III. VERIFICATION OF THE METHOD USING A HOLLOW CYLINDRICAL SHELL

In view of the above development, the bi-static RCS of surface can be obtained in terms of the scattering amplitude as follows [8-10]:

$$\sigma_{pq} = 4\pi\,|\,f_{pq}(\mathbf{o},\mathbf{i})\,|^2. \quad (12)$$

Notice from (9) and (10) that f_{pq} depends on the shape (S), and the dielectric properties of scatterer. Both functions depend on the orientation of the scatterer, but S generally varies much more rapidly than other functions in f_{pq}.

Using the developed method, the scattering amplitudes of circular hollow finite length discrete cylindrical shell with length l as seen in Fig. 2., are found as:

$$f_{pq} = \frac{{k_0}^2 T}{4\pi}\left\{\mathbf{p}\cdot\mathbf{q}\sum_{c=1}^{N}(\varepsilon_r - 1)e^{jk_0\boldsymbol{\zeta}\cdot\mathbf{r}_c}S_m^{(c)} - \sum_{c=1}^{N}\frac{(\varepsilon_r - 1)^2}{\varepsilon_r}(\mathbf{p}\cdot\mathbf{n_c})\,(\mathbf{n_c}\cdot\mathbf{q})\,e^{jk_0\boldsymbol{\zeta}\cdot\mathbf{r}_c}S_m^{(c)}\right\}, \quad (13)$$

with $\boldsymbol{\zeta}\cdot\mathbf{r}_c = a\zeta_y + a(\zeta_y\cos\varphi + \zeta_z\sin\varphi)$, a is the inner radius of the cylinder, φ is the angle which is measured from x axis, and T is the thickness. Next converting the sum, (13) becomes;

$$f_{hh} = \frac{{k_0}^2(\varepsilon_r - 1)Tl}{4\pi}\left\{h_{is}s_1 - \frac{\varepsilon_r - 1}{\varepsilon_r}(h_1 s_2 + h_2 s_3 + h_3 s_4)\right\}, \quad (14)$$

$$f_{vv} = \frac{{k_0}^2(\varepsilon_r - 1)Tl}{4\pi}\left\{v_{is}s_1 - \frac{\varepsilon_r - 1}{\varepsilon_r}(v_1 s_2 + v_2 s_3 + v_3 s_4)\right\}. \quad (15)$$

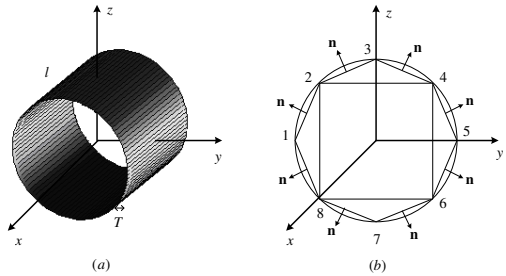

Fig. 2. (a) 3D Discretized cylinder shell and (b) exaggerated cross section.

The parameters, which appear in (14) and (15) are given in Appendix. Comparison of (14) and (15) with [10] shows very good agreement and summations in equations yield the Bessel function of the first kind as expected. This is the proof of discretization of the hollow finite length cylindrical shell. Equations (14) and (15) give the same RCS in [10] and in the limit of low frequencies as in [8].

We also verify our numerical result with the exact results of [11] by inverting their two dimensional results to three dimensional radar cross-sections (σ_{3D}) using the following formula [12],

$$\sigma_{3D} = \sigma_{2D}\frac{2l^2}{\lambda}, \quad (16)$$

where λ is the wavelength and σ_{2D} is two dimensional RCS. In [11], the theoretical scattering solution for plane wave incident normally on a lossy dielectric multilayer

circular cylinder of infinite length is outlined, and the two dimensional exact RCS are given as

$$\sigma_{2D} = \frac{4}{k_0} |T_p(\varphi)|^2 , \qquad (17)$$

where

$$T_p(\varphi) = \sum_{n=0}^{\infty} e_n D_n^{(p)} \cos(n\varphi) , \quad p \in \{h, v\} \qquad (18)$$

with $e_n = 1$ for $n = 0$, $e_n = 2$ for $n = 1, 2, \ldots$.

Next as a part of the study, the bi-static RCS of cylindrical surface with $\varepsilon_r = 29.1 - j13.3$, radius $a = 27.5$ cm, thickness $T = 0.2$ mm, length $l = 1$ m, and $f = 900$ MHz was computed by using (12). The results were compared with those obtained by using the exact solution (16) for verification [11]. Figures 3 and 4 clearly show that the solution obtained for cylinder by developed discretizing method approaches very closely to exact results for horizontal and vertical polarization.

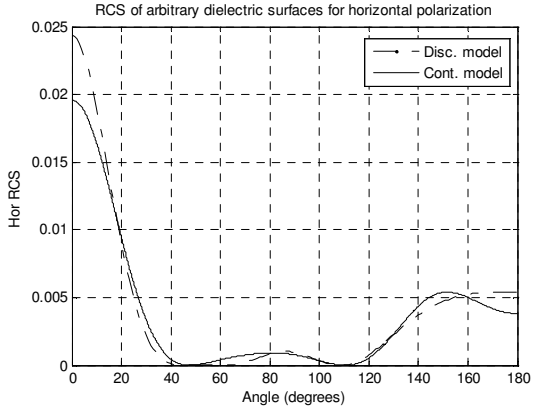

Fig. 3. RCS for horizontal polarization at 900MHz.

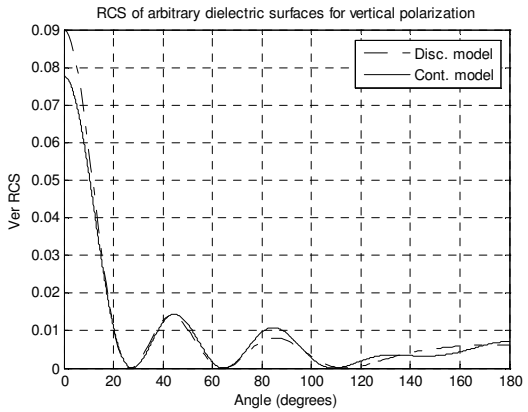

Fig. 4. RCS for vertical polarization at 900 MHz.

IV. SIMULATION RESULTS OF A TUNNEL

In this part, as a further proof of the method, attenuation in a tunnel was simulated by a cylindrical shell as seen in Fig. 2. We have run our simulation program and compared with the measurements, which were done in Berlin Subway system [6]. In our simulation, the tunnel cross section was modeled by a different cross sectional shapes. Statistical packet like spline routine provides necessary extra points for good accuracy. If the cross section is rectangular then all the strips in Fig. 2 taken between the points 8-2, 2-4, 4-6, and 6-8 are located along the line. If the cross section is open-grove then the normal vectors of strips along the points 2-4 are taken as a zero. The length of the configuration does not have to be constant; it can be variable as well. The building material was given to be dry concrete with $\varepsilon_r = 5 - j0.1$.

Figures 5 and 6 show the simulation results of our model. Figure 5 depicts the tunnel cross section as modeled by a circle with elevated floor. Figure 6 depicts rectangular cross section of width $w = 5.25$ m and height $h = 4.28$ m. The thickness of the wall is taken as 20 cm. Several different layers can be used in the simulation where necessary.

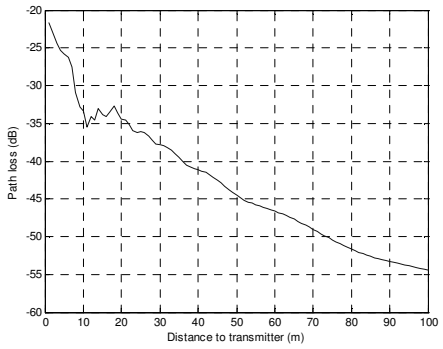

Fig. 5. The simulation results for $f = 1800$ MHz, $\varepsilon_r = 5 - j0.1$ arched cross-section.

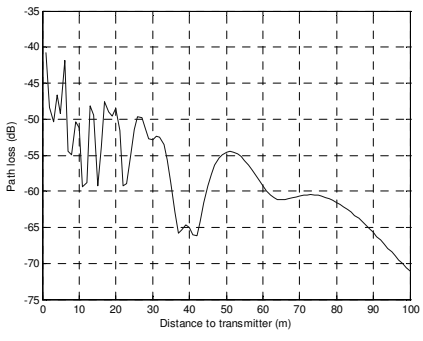

Fig. 6. The simulation results for $f = 1800$ MHz, $\varepsilon_r = 5 - j0.1$ rectangular cross-section.

The comparison between the results of discrete model with literature shows that the results of the simulation are indeed very close to measured values. The general shapes of the curves (considering the mean curve in figures) are exactly the same. They are both monotonically decreasing curves. They share the same range of values for attenuation.

Once again, depending on the ratio between the transverse dimensions of the tunnels and wavelength and on the distance from the transmitter, the attenuation values can be either greater or smaller than the attenuation in free-space. Curves in Figs. 5 and 6 clearly show this phenomenon.

In evaluating the results, it should also be noticed that the real world measurements involve many incident rays at different angles of interference simultaneously. The possible constructive and destructive interference between different plane waves is ignored. This also contributes to the differences between the measurement and simulation curves. The simulations reveal that the correct modeling parameter of the tunnel's cross-section influences the accuracy of the modeling results.

V. DEVELOPMENT OF MODEL FOR THE URBAN AREAS

In the real world, there are many objects, walls with windows and door, and gaps on the streets that contribute to the loss of electromagnetic wave at the receiver point. If we want to model buildings in the urban areas, we have to take into account these contributions to get reasonable results. Thus, actual discretization must be as seen in Fig. 7. In order to verify the model, windows, openings etc. are not taken into consideration in the following simulations.

Now, we will enhance our model to use it in urban areas, which have both side walls and slits (gaps between side walls). The walls and streets are modeled as a multilayer thin rectangular plate.

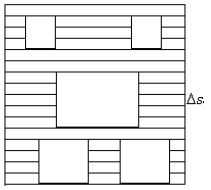

Fig. 7. The discretized wall of building.

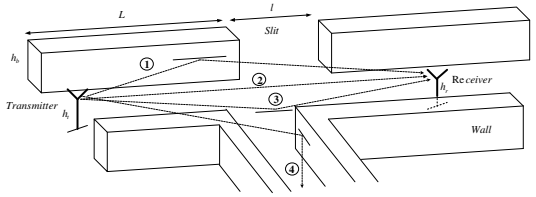

Fig. 8. 3D Illustration of urban areas.

As seen in Fig. 8, the total field density at the receiver is the sum of several rays, which are scattered from the inner side of walls (no windows) and smooth ground. But, our model can handle walls with windows and a door, and ground with holes or irregularities. Since the antennas' height is lower than the rooftop level the diffraction from the roof edges has been omitted.

Some of the parameters seen in the figure are h_t transmitter height, h_r receiver height, h_b average building height, l length of slits, and L length of sidewalls. Waves 1 and 3 can reach to the receiver antenna trough the wall and ground respectively. Wave 4 cannot reach to receiver and gets lost in the side streets.

Only single scattering (first order) from the walls and ground is illustrated in the Fig. 8. However, we know that the second and third order scattering also contribute to the field density. Therefore, we have added these contributions to our calculation. After the third scattering, the loss of electric field increases so much that the contribution of this multiple scattered waves can be neglected.

As seen from the Fig. 8 some of the waves cannot reach to the receiver antenna as wave 4 does. Therefore, we have to choose the waves that can reach the antenna in order to find the total field. Scattering from the walls is taken into account by introducing the special brokenness parameter χ in terms of slit length of l_i and length of sidewalls L_i as presented in [1]

$$\chi = \frac{L_i}{L_i + l_i} \qquad (i = 1,2...) . \tag{19}$$

The magnitude of χ shows the density of the buildings and takes the value between 1 and 0 $(0 \le \chi \le 1)$. If χ is "0", it means there is no side wall. The result must be equal to the loss of free space. If χ is "1", there are no slits or any gaps . As a result the following can be written:

$$\chi = \begin{cases} 1 \;\; \text{AT} = \text{Loss for no gap} \\ 0 \;\; \text{AT} = \text{Loss for no sidewall (free space)} \end{cases}, \tag{20}$$

where AT is the total attenuation at receiver antenna.

In the developed software we moved the receiver antenna along the street and computed average total electric field for certain distances from the transmitter for both broken and unbroken models. Then, we calculated the path loss along the street for the LOS conditions. Finally, we developed the following field attenuation equation:

$$\text{AT} = \text{AT}_{\text{unbrk}} + (\text{AT}_{\text{open}} - \text{AT}_{\text{unbrk}}) \times (1 - \chi) , \tag{21}$$

where AT_{unbrk} represents attenuation at no gap, and AT_{open} represents free space attenuation. We have chosen the parameter χ according to the density of the buildings in the referenced surveys.

Next, we will present the some simulation results, which was done using the parameters from the literature such as street width, brokenness parameter, dielectric properties of the buildings etc.

VI. THE SIMULATION OF WAVE PROPAGATION FOR THE URBAN AREAS

We have run our software for the study of Open-Groove Structures for verification as seen in Fig. 9. Following parameters have been used for the simulation: $f = 2\,\text{GHz}$, $\varepsilon_r = 4.18$, $\sigma = 0.026\,S/m$ as stated in [4]. These dimensions have also been divided into small sheets as depicted in Fig. 7, in order to find the scattering amplitudes of each strip and total electric fields.

We obtained separate solutions for the vertical and horizontal field density in Fig. 10. Horizontal scale represents distance from the source in meter. We can see from the figures that the path loss is increasing with increasing distance. The path loss for horizontal polarization is more than the one for vertical polarization.

The second simulation has been done for the experimental data presented in [13] for conditions of direct visibility along streets in Manhattan, New York. We used the same parameters of measurement as presented in [13] such as $h_b = 50\,\text{m}$ for average building heights, $f = 900\,\text{MHz}$ for the operating frequency, $a = 30\,\text{m}$ for the street width, $\varepsilon_r = 15$, $\sigma = 7$ for dielectric properties of the sidewalls, and χ=0.8. The output of the simulation is illustrated in Fig. 11.

The graph reveals that the output highly depends on the shape of the streets and the more the shape is uncertain, the more difficult it is to get an accurate result. As we add the slits to our model, the waves at receiver antenna decrease. This leads to lower signal power at receiver point.

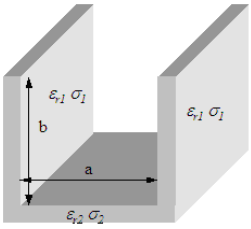

Fig. 9. 3D Cross section of open-groove structure.

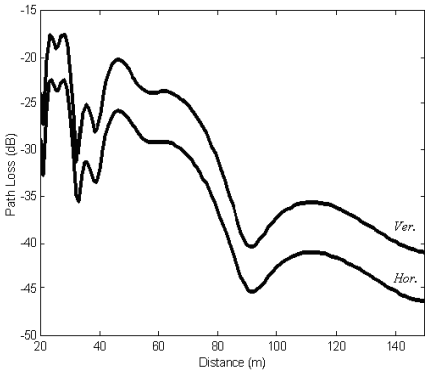

Fig. 10. The simulation results of open groove structure for horizontal and vertical polarization.

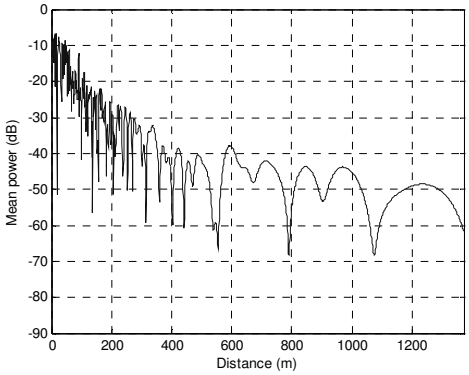

Fig. 11. The simulation results for New York City.

The result of our simulation follows the experimental results staying 10 dB below them. This is due to the contribution of the scattered waves from the other objects in the street. Also the dielectric properties of the buildings, vehicles and unexpected objects affect the total signal power at the receiver.

The following is the simulation result for the small town of Kefar–Yona, Israel [2]. The values for the scattering parameters used in the simulation are $h_b = 10\,\text{m}$ for average building heights, $f = 900\,\text{MHz}$ for the operating frequency, a=50m for the street width, $\varepsilon_r = 15$, $\sigma = 7$ for dielectric constant and conductivity of the sidewalls. The wall thickness is taken as 20 cm. In order to describe the density of the buildings in the brokenness parameter has been defined in the experimental result in the survey. These parameters were used in our simulation. Then, using 20 cm thickness as a model of vegetation canopy is added to the wall. The effect of these layers is investigated. We have found good results for relative signal loss. The signal loss shows the field intensity attenuation, which is relative to the intensity in free space at the distance 100m from the source, as it is done in the study. We have calculated up

to three scatterings from the walls and ground, which are quite close to approximate result. Higher orders do not contribute to the result more than 1 per cent.

The curves in Fig. 12, show our simulation results for urban area with and without vegetation canopy respectively. Our model gives results, which are close to experimental data [2] and can be used for predicting path loss distributions along the street. The effect of plant for signal loss causes 3-5 dB increase in simulation.

We have also run our simulation program for different environmental conditions in the city scene. We have assumed New York streets flooded and used the electric properties of fresh water and calculated the power loss of EM waves. We have used the electrical properties of asphalt in the normal condition which is $\varepsilon_r = 4.28 + j0.1$ [14-15]. The electrical properties of the fresh water are assumed as $\varepsilon_r = 81$ and $\sigma = 0.01$ [9]. Figure 13 depicts the comparison of the two cases using our model. As seen in the figure the electrical properties of the ground surface affects the power loss in the city streets. It can be inferred from this figure that the power loss decreases when the ground gets wet. Finally, we have studied loss in New York City for different brokenness parameters. We have found the following LOS contributions for different brokenness parameters.

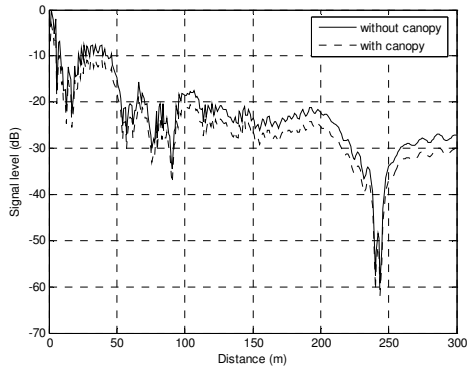

Fig. 12. The simulation result for urban area.

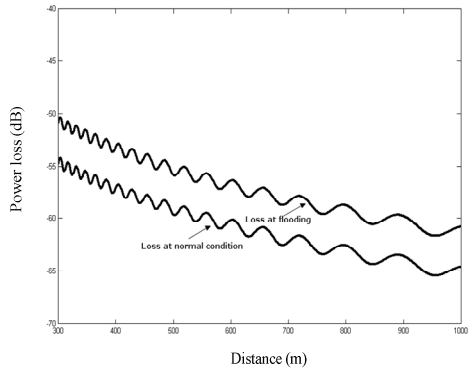

Fig. 13. Power loss of asphalt and flooded surface.

Table 1: LOS contributions of brokenness parameters.

χ	LOS contribution (in per cent)
0	100
0.4	63
0.8	40
1	32

VII. CONCLUSIONS

In this study, a new theoretical model based on the discretized properties of lossy dielectric arbitrary surfaces was developed using scattering theory. Firstly, the model is used to simulate RCS and the attenuation characteristics of EM waves. The simulation results were compared to the values in the literature and it was seen that the model agrees well with them. In our calculation we observed that in the total field, the effect of the first and second order-scattered waves are approximately 20-25 and 10 per cent respectively. After the third order scattering, the contribution of higher orders decreases so that the effect of these waves can be neglected. Direct wave, which reaches (LOS condition) to the receiver antenna is 50-60 per cent. We enhanced the new theoretical model in order to study wave propagation in urban environments for mobile applications and compared with the previous studies to verify our model.

In our developed model, the total field density in the observed point is calculated by adding the line-of-sight and scattered wave contributions from the walls. Furthermore, higher order scattered waves can also be calculated.

The developed discrete model has the following unique advantages over the earlier propagation models :

1. It is possible to calculate the contributions of each direct (LOS) and scattered waves separately. It accounts for the scattering from the walls with/without openings and ground (dry or wet) with holes and irregularities, as well as gaps between the buildings.
2. The developed model is applicable for a broad band of frequencies.
3. If the shape of the urban areas is entered to the simulation program with sufficient detail, the output gets very close to the measurement results. Even when the shape is not entered very accurately; an approximate result can be obtained.
4. This model can be used effectively for prediction of loss characteristics in a situation where two antennas are located below the roof tops in conditions of direct visibility at the ranges more than 150-200 m.
5. The proposed physical propagation model will be useful for describing urban propagation channels and can be extended to more complicated configurations including additional factors affecting the radio wave propagation.

VIII. ACKNOWLEDGEMENTS

This work is supported by Bogazici University Research Foundation (Project No;BAP03A207).

REFERENCES

[1] N. Blaunstein, *Radio Propagation in Cellular Network*, Artech House Inc, Boston-London, 2000.

[2] N. Blaunstein, "Average field attenuation in the nonregular impedance street waveguide," *IEEE Trans. on Anennas and Propagation*, vol. 64, pp. 1782-1788, Dec. 1998.

[3] J. Walfisch and H. L. Bertoni, "A theoretical model of UHF propagation in urban environments," *IEEE Trans. on Antennas and Propagation*, vol. AP-36, pp. 1788-1796, Dec. 1988.

[4] Y. P. Zhang, Y. Hwang, and J. D. Parsons, "UHF radio propagation characteristics in a straight open-groove structures," *IEEE Trans. on Vehicular Technology*, vol. 48, no. 1, pp. 249-254, Jan. 1999.

[5] European Communities, COST231 Final Report, Digital Mobile Radio Toward Future Generation Systems, pp. 115-208, 1999.

[6] D. Didascalou, Y. Venot, M. Döttling, and W. Wiesbeck, "Modeling and measurements of EM-wave propagation in the Berlin Subway," *in Millenium Conference on Antennas&Propagation AP2000*, Davos, Switzerland, April 2000.

[7] S. S. Seker and B. Altay, "Shielding properties of thin curved surfaces," *Proc. IEEE EMC-96*, Santa Clara, USA, 1996.

[8] S. S. Seker, "Radar cross section of thin dielectric bodies," *Proc. IEE*, vol. 133(4), pp 305-307, Aug. 1986.

[9] D. Paris and K. Hurd, *Basic Electromagnetic Theory*, Mc Graw Hill Book Company, 1969.

[10] G. Ruck, D. Barrick, W. Stuart, and C. Krichbaum, *Radar Cross-Section Handbook*, vol 1, Plenum Press, New York, 1970.

[11] H. Bussey and J. Richmond, "Scattering by a lossy dielectric circular cylindrical multilayer numerical values," *IEEE Trans. on Antennas and Prop.*, vol. 23, no. 5, pp. 723-725, Sep. 1975.

[12] C. Balanis, *Advanced Engineering Electromagnetics*, Wiley and Sons, pp. 578, 1989.

[13] A. J. Rustako, N. Amitay, G. J. Owens, and R. S. Roman, "Radio propagation at microwave frequencies for line-of-sight microcellular mobile and personal communications," *IEEE Trans. on Veh. Tech.*, vol. 40, no. 1, pp. 203-210, Feb. 1991.

[14] ERADS, "Expert Radar Signature Solutions, Common Radar Materials" from World Wide Web < http://stl.uml.edu/tools/scalemodel.html>.

[15] J. Wait, *Wave Propagation Theory*, Pergamon Press, New York, 1981.

APPENDIX

The parameters of (14) and (15) are given as:

$v_{is} = (v_1 + v_2) + \sin\theta_i \sin\theta_s$, $v_1 = \cos\theta_s \cos\phi_s \cos\theta_i \cos\phi_i$

$v_2 = \cos\theta_s \sin\phi_s \cos\theta_i \sin\phi_i$, $h_1 = -\sin\phi_i \sin\phi_s$

$v_3 = 0.5\sin(\phi_i + \phi_s)\cos\theta_s \cos\theta_i$, $h_2 = -\cos\phi_i \cos\phi_s$,

$h_{is} = (h_1 + h_2) = -\cos(\phi_i - \phi_s)$, $h_3 = 0.5\sin(\phi_i + \phi_s)$,

$s_1 = 2\pi a_1 J_0(x_1)$, $s_2 = \pi a_1\left[J_0(x_1) - J_2(x_1)\cos(2\psi)\right]$,

$s_3 = \pi a_1\left[J_0(x_1) + J_2(x_1)\cos(2\psi)\right]$

$s_4 = -2\pi a_1\left[J_2(x_1)\sin(2\psi)\right]$ with $x_1 = k_0 a_1\sqrt{\gamma_x^2 + \gamma_y^2}$,

$\psi = \tan^{-1}(\gamma_y / \gamma_x)$. In the above equations $J_0(x_1)$ and $J_2(x_1)$ represent Bessel function of the first kind, zero and the second order respectively.

Selim Seker received his MS and PhD degrees in 1978 and 1982 from the George Washington University, D.C., USA. He has been working in the area of microwave remote sensing, propagation and biological effect of EM. Fields and related areas. In the summer of 1983-85 and 1987 as well as between 1982 to 1983 he was with CyberCom Co., VA, USA and conducted research in the area of EM propagation through forests. In summer of 1986, he worked on the problem of EM scattering and absorbers at BBC Baden Switzerland. On his sabbatical leave 1990-1992, he taught several different courses at both graduate and undergraduate level at GWU, and conducted one year theoretical and experimental research for NASA. He has published several journal and conference papers in the area of EM wave propagation. He is a senior member of IEEE.

Gökhan Apaydin was born in Ankara, Turkey, in 1978. He received his BS, MS, and PhD degrees in Electrical and Electronic Engineering, from Bogazici University, Istanbul, Turkey in 2001, 2003, and 2007 respectively. He was employed by Bogazici University between 2001 and 2006. He has been a research engineer at University of Technology Zurich applied R&D since 2005. He has been working several research projects on EM scattering, the development of Finite Element Method for electromagnetic computation, propagation, web-splines, positioning, RFID applications, filter design, wavelet and related areas. He has published 3 journal papers and presented 11 conference papers. He is also the author of many technical reports and research books at University of Applied Science Zurich. He is a member of IEEE.